

# **The Improved Efficiency of Quantum-Dot-Sensitized Solar Cells with a Wide Spectrum and Pure Inorganic Donor-Acceptor Type Polyoxometalate as a Collaborative Cosensitizer**

Li Chen,<sup>a</sup> Weilin Chen,<sup>a\*</sup> Huaqiao Tan,<sup>a</sup> Jiansheng Li,<sup>b</sup> Xiaojing Sang,<sup>b</sup> and Enbo Wang <sup>a\*</sup>

<sup>a</sup> Key Laboratory of Polyoxometalate Science of Ministry of Education, Department of Chemistry, Northeast Normal University, Changchun, Jilin 130024, China

<sup>b</sup> School of Chemistry and Chemical Engineering, Liaoning Normal University, Dalian 116029, China

## **CONTENTS**

### **Supplementary Physical and Chemical Characterizations**

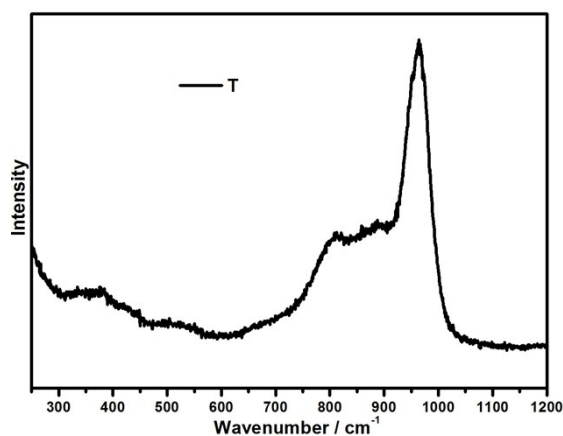


Fig. S1 The normal Raman spectrum for T.

Raman spectrum, which was studied as a kind of scattering spectrum, could provide the structure of POMs by researching their vibration and rotation energy. In the Fig. S1, the bands from 800-900 cm<sup>-1</sup> were associated with the stretching mode of W-O<sub>b</sub>-W or W-O<sub>c</sub>-W and 900-1000 cm<sup>-1</sup> were associated with the stretching mode of W-O<sub>t</sub>. Beyond that the lower energy regions were associated with the bending mode of W-Ob-W or W-Oc-W or Si-O. Therefore the normal Raman spectrum can confirm the structure of prepared T.

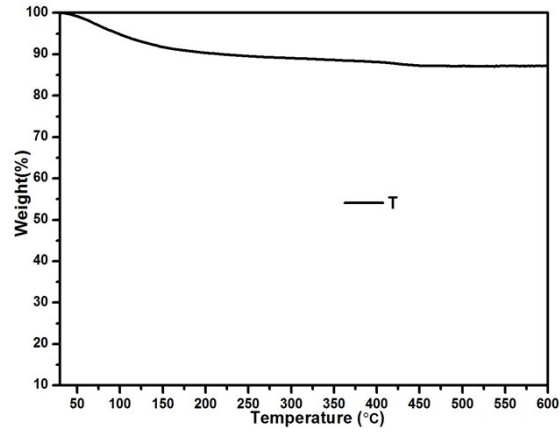


Fig. S2 TG curve of T. The thermal stability of T was analyzed by its TG curve, which displayed three-step weightlosses occurred in the temperature range of 50-600°C. The three-step weightlosses were all attributed to the loss of water.

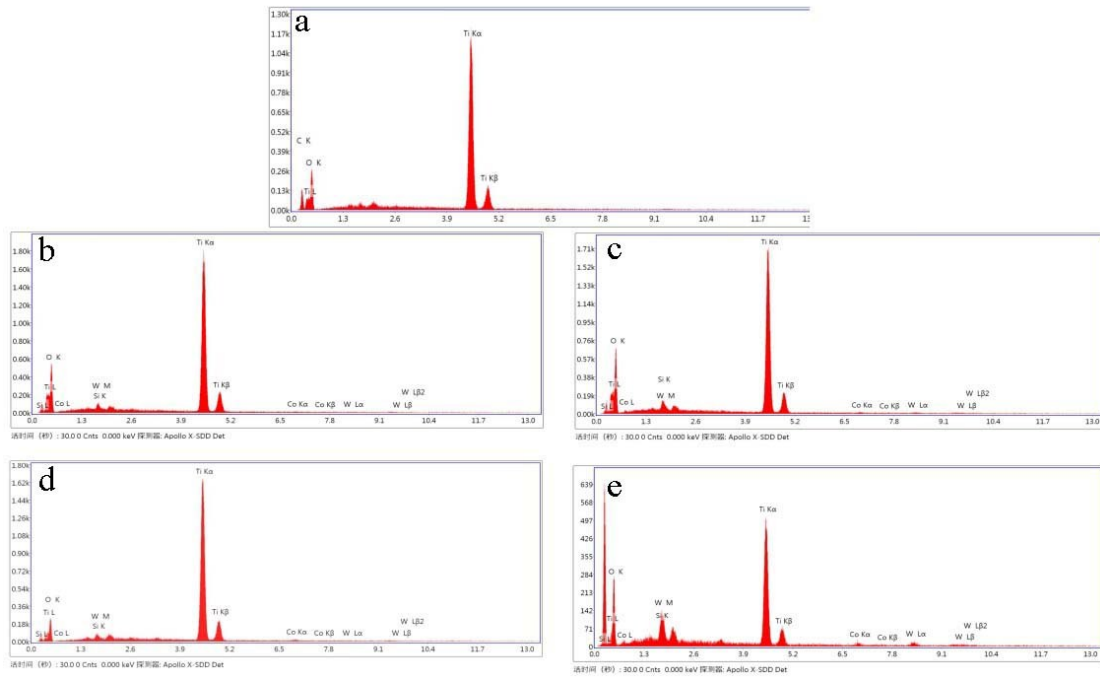


Fig. S3 EDS spectrum for a) pure  $\text{TiO}_2$ ; b)  $\text{T1@TiO}_2$ ; c)  $\text{T2@TiO}_2$ ; d)  $\text{T3@TiO}_2$ ; f)  $\text{T4@TiO}_2$ .

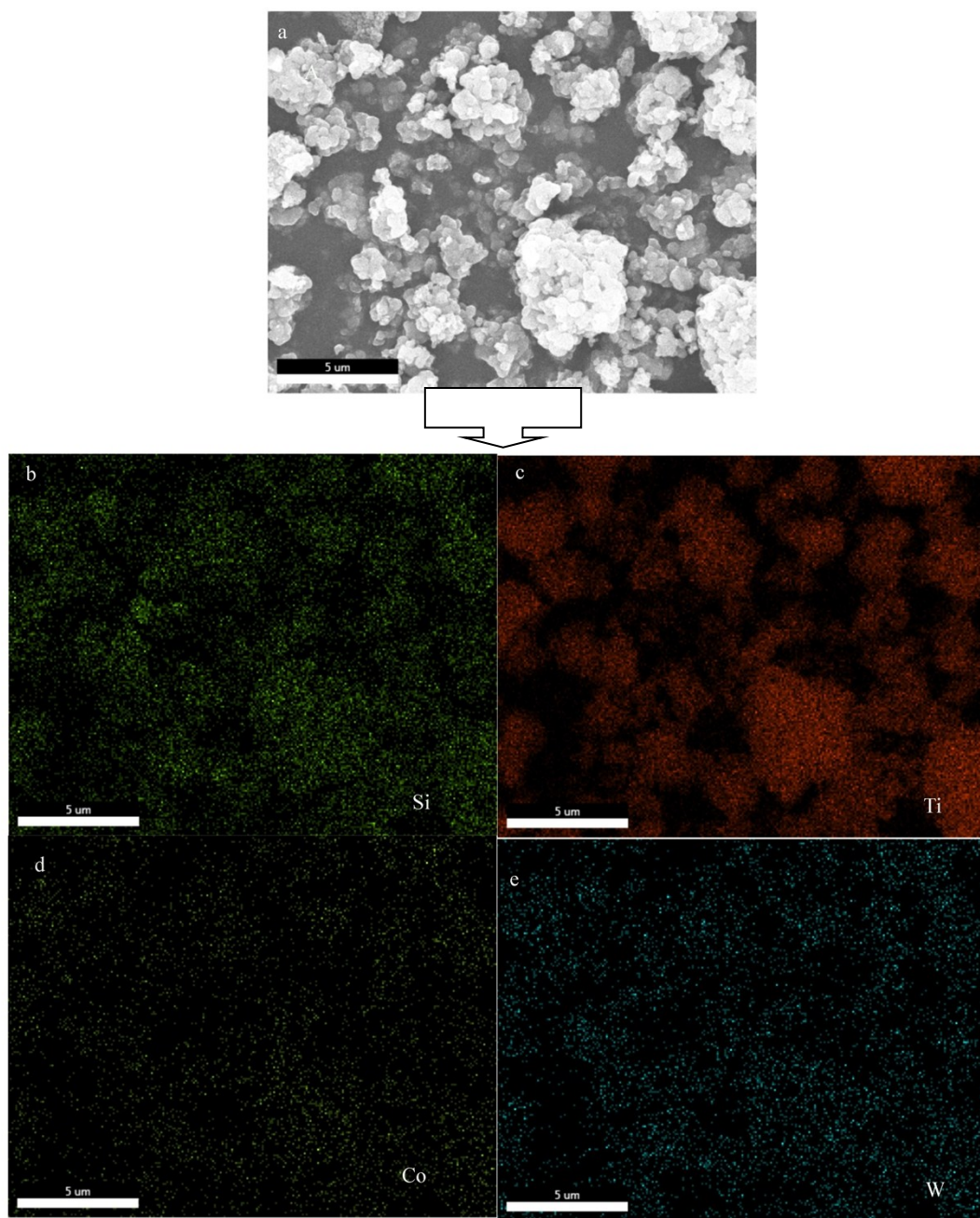


Fig. S4 Element mapping of T3@TiO<sub>2</sub> powder: a) the SEM image of the T2@TiO<sub>2</sub>; b) the element mapping of Si; c) the element mapping of Ti; d) the element mapping of Co; f) the element mapping of W.

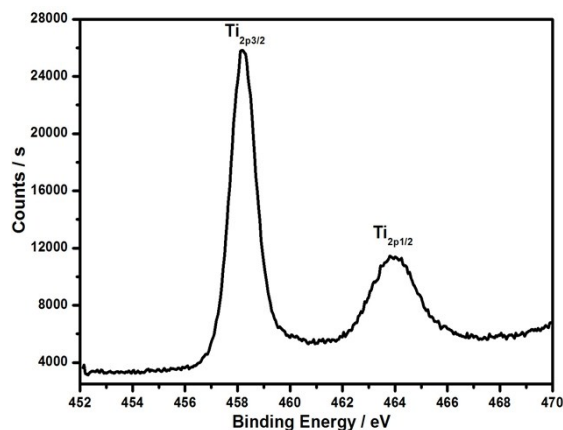


Fig. S5 The X-ray photoelectron spectroscopy of Ti of T3@TiO<sub>2</sub>. The Fig. S5 exhibits two peaks at ca. 458.2 eV in the energy region of Ti<sub>2p3/2</sub> and ca. 463.9 eV in the energy region of Ti<sub>2p1/2</sub>, which are consistent with the Ti<sup>IV</sup> oxidation state.<sup>S1</sup>

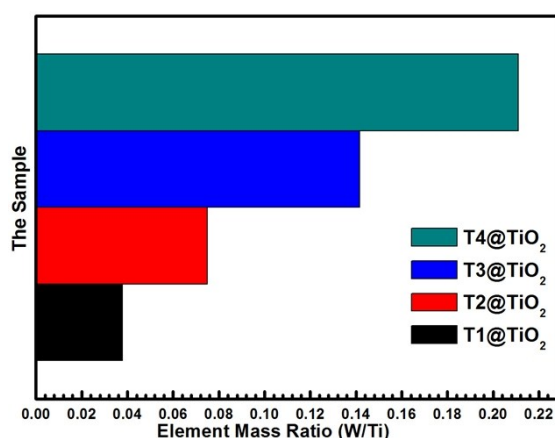


Fig. S6 The elemental mass ratio of W/Ti in T1@TiO<sub>2</sub>, T2@TiO<sub>2</sub>, T3@TiO<sub>2</sub>, T4@TiO<sub>2</sub>. The loading amount of T in the composites was determined by inductively coupled plasma atomic emission spectrometer(ICP-AES), from which the W content in composites was 3.78%, 7.49%, 14.17%, 21.10% respectively.

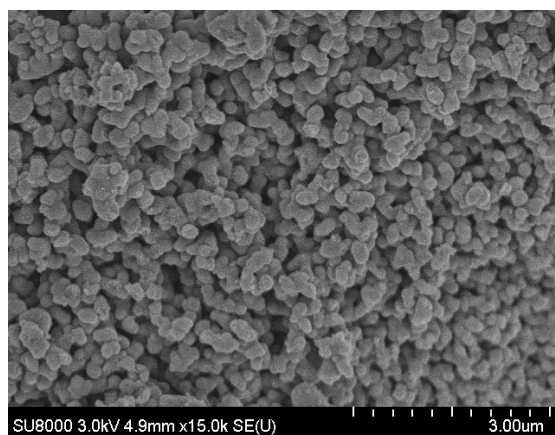


Fig. S7 The SEM images of the prepared T2@TiO<sub>2</sub> under the low multiples.

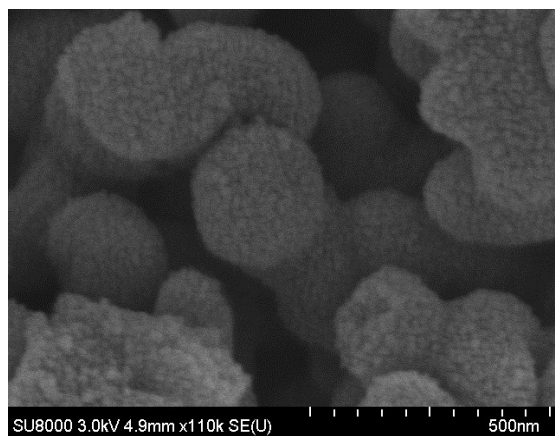


Fig. S8 The SEM images of the prepared T2@TiO<sub>2</sub> under the high multiples.

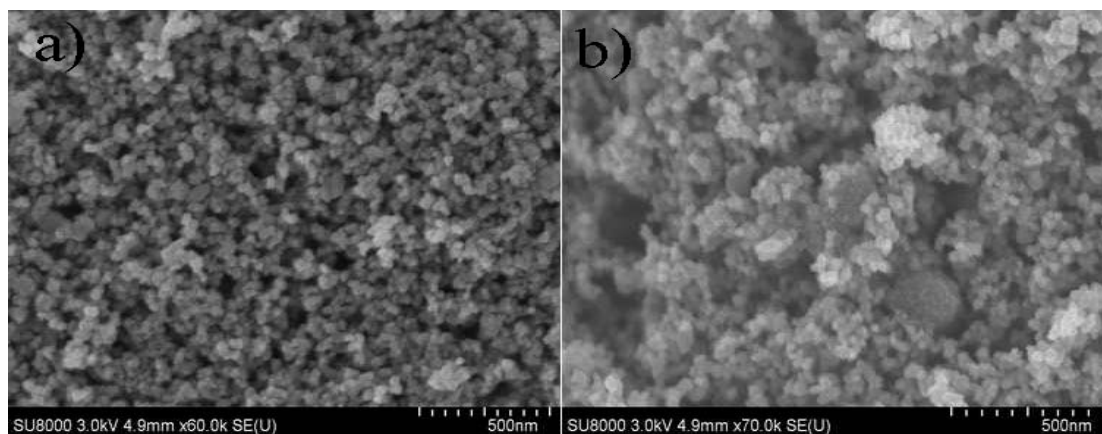


Fig. S9 The SEM images of different photoanode films: a) pure  $\text{TiO}_2$  film; b)  $\text{T3@TiO}_2$  film, which showed that pure  $\text{TiO}_2$  film consisted of uniform  $\text{TiO}_2$  particles, whereas  $\text{T2@TiO}_2$ -doped film contained some agminated micropore ball.

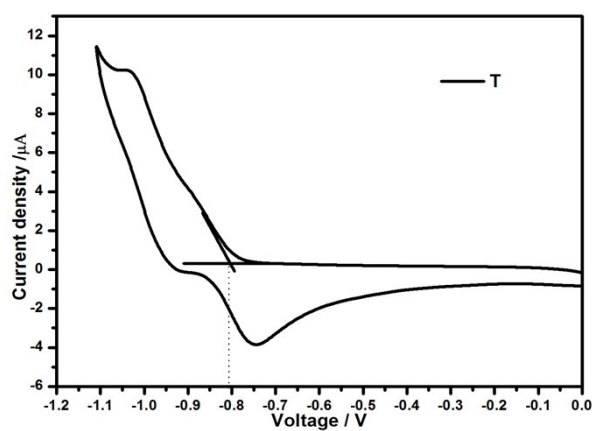


Fig. S10 Cyclic voltammetry curve of the T in 0.5M HAc/NaAc buffer solution with  $\text{pH} = 6.00$  in the voltage range from 0 V to -1.2 V

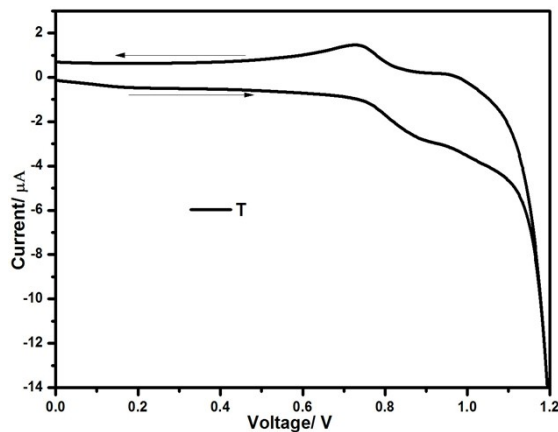


Fig. S11 Cyclic voltammetry curve of the T in 0.5M HAc/NaAc buffer solution with pH =6.00 in the voltage range from 0V to 1.2V .

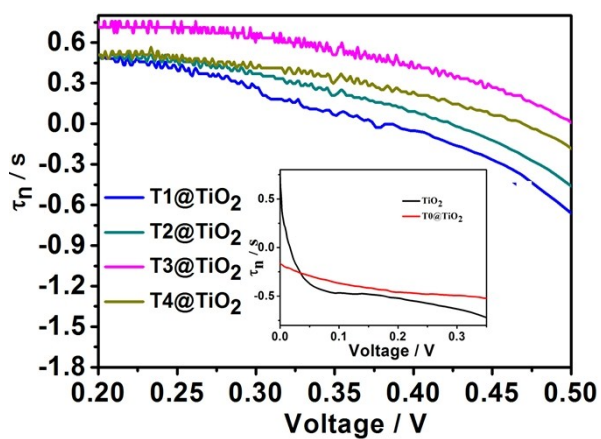


Fig. S12 the electron lifetime calculated from OCVD of CdSe sensitized T1@TiO<sub>2</sub>, T2@TiO<sub>2</sub>, T3@TiO<sub>2</sub> and T4@TiO<sub>2</sub> cells; the Inset) the electron lifetime calculated from OCVD of CdSe sensitized pure TiO<sub>2</sub> and T0@TiO<sub>2</sub> cells.



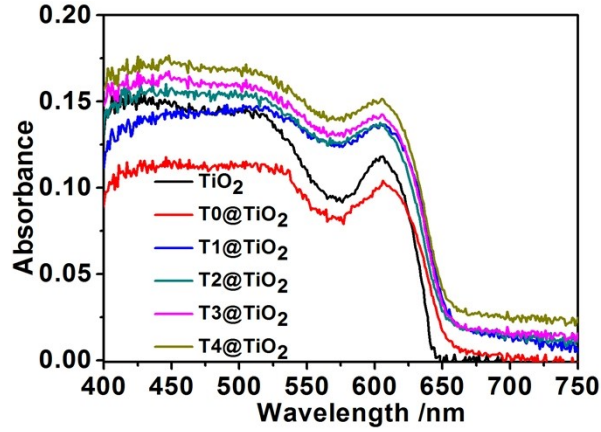


Fig. S13 UV-vis absorption spectra of CdSe sensitized pure  $\text{TiO}_2$  and  $\text{T@TiO}_2$  photoanode films after deposition for 6h.

Absorption spectra of CdSe sensitized pure  $\text{TiO}_2$  and  $\text{T@TiO}_2$  photoanode films were shown in Fig. S13. As can be seen from the Fig. S13, the absorbance of CdSe sensitized  $\text{T0@TiO}_2$  photoanode films are slightly larger than the CdSe sensitized pure  $\text{TiO}_2$  photoanode films. The possible reason is that the large particles of  $\text{TiO}_2$  are conducive to the absorption of the spectrum. Furthermore, the absorbance of CdSe sensitized  $\text{T@TiO}_2$  ( $\text{T1@TiO}_2$ ,  $\text{T2@TiO}_2$ ,  $\text{T3@TiO}_2$ ,  $\text{T4@TiO}_2$ ) photoanode films increased with the increase of the content of T. And the absorbance of CdSe sensitized  $\text{T@TiO}_2$  ( $\text{T1@TiO}_2$ ,  $\text{T2@TiO}_2$ ,  $\text{T3@TiO}_2$ ,  $\text{T4@TiO}_2$ ) photoanode films are obvious wider than the CdSe sensitized pure  $\text{TiO}_2$  photoanode films in the range from the 550 to 600nm and after 650nm. Experimental results show that T added to the photoanodes as collaborative cosensitizer can constitute a wider spectrum of absorption.

Table S1 Simulated values of resistance ( $R_{\text{rec}}$ ) and capacitance ( $C_{\mu}$ ) for cell devices based on CdSe sensitized pure  $\text{TiO}_2$  and T@ $\text{TiO}_2$  photoanodes at the forward bias of  $-0.60\text{ V}$ .

Cells	$\text{TiO}_2$	T0@ $\text{TiO}_2$	T1@ $\text{TiO}_2$	T2@ $\text{TiO}_2$	T3@ $\text{TiO}_2$	T4@ $\text{TiO}_2$
$R_{\text{rec}}/\Omega\text{ cm}^{-2}$	49	65	153	254	310	144
$C_{\mu}/\text{mF cm}^{-2}$	3.21	3.23	3.31	3.39	3.27	3.18

## References

- S1 M. Vasilopoulou, A. M. Douvas, L. C. Palilis, S. Kennou, and P. Argitis, *J. Am. Chem. Soc.* 2015, **137**, 6844–6856.